

Evidence for a $k^{-5/3}$ spectrum from the EOLE Lagrangian balloons in the low stratosphere

Guglielmo Lacorata¹, Erik Aurell², Bernard Legras³ and Angelo Vulpiani⁴

¹*CNR, Institute for Atmospheric and Climate Sciences, Lecce, Italy*

²*KTH Royal Institute of Technology,*

Department of Physics, Stockholm, Sweden

³*Ecole Normale Supérieure, Laboratoire de*

Météorologie Dynamique, UMR8539, Paris, France and

⁴*University of Rome "La Sapienza", Department of Physics, and*

INFM (UdR and SMC), Rome, Italy

ABSTRACT

The EOLE Experiment is revisited to study turbulent processes in the lower stratosphere circulation from a Lagrangian viewpoint and resolve a discrepancy on the slope of the atmospheric energy spectrum between the work of Morel and Larchevêque (1974) and recent studies using aircraft data. Relative dispersion of balloon pairs is studied by calculating the Finite Scale Lyapunov Exponent, an exit time-based technique which is particularly efficient in cases where processes with different spatial scales are interfering. Our main result is to reconcile the EOLE dataset with recent studies supporting a $k^{-5/3}$ energy spectrum in the range 100-1000 km. Our results also show exponential separation at smaller scale, with characteristic time of order 1 day, and agree with the standard diffusion of about $10^7 \text{ m}^2\text{s}^{-1}$ at large scales. A still open question is the origin of a $k^{-5/3}$ spectrum in the mesoscale range, between 100 and 1000 km.

I. INTRODUCTION

The EOLE project consisted in the release of 483 constant-volume pressurized balloons, in the Southern Hemisphere mid-latitudes throughout the period September 1971-March 1972, at approximately 200 hPa. The life-time of these balloons was from a few days to about one year, with an average value of about 120 days. Their motion was basically isopycnal except for small diurnal volume variations of the envelop of less than 1% and inertial oscillations of a few meters in the vertical, excited by wind shear and small-scale turbulence. The position of the balloons and meteorological parameters were periodically transmitted to satellite by ARGOS system. The trajectories of the EOLE experiment still provide nowadays the most extensive data set of experimental quasi-Lagrangian tracers in the atmosphere for observing the properties of the medium-to-large-scale motion at the tropopause level.

Both Eulerian and Lagrangian analyses have been performed by several authors. Morel and Desbois (1974) deduced the mean circulation around 200 hPa from the balloon flights, as formed by a mid-latitude zonal stream with a meridional profile characterized by a typical velocity $\sim 30 \text{ ms}^{-1}$ inside the jet, overimposed to meridional velocity field disturbances of much smaller intensity, $\sim 1 \text{ ms}^{-1}$, and to residual standing waves acting as spatial perturbations of the zonal velocity pattern, producing the typical shape of a meandering jet. These results have been largely confirmed by operational analysis since then. Morel and Larchevêque (1974), hereafter ML, investigated the synoptic-scale turbulent properties. They measured the mean square relative velocity and the relative diffusivity of balloon pairs, and found essentially two major regimes for Lagrangian dispersion: exponential separation for time delays less than 6 days and standard diffusion for larger times. These authors also observed that the scaling of the relative diffusivity with the separation length between two balloons agreed with a direct 2D turbulent cascade, with energy spectrum $E(k) \sim k^{-3}$, or steeper, in the range 100-1000 km. Further Eulerian analyses of large-scale velocity spectra by Desbois (1975) were compatible with the scenario proposed by Morel and Larchevêque (1974) about isotropic and homogeneous 2D turbulence with a k^{-3} energy distribution up to scales $\sim 1000 \text{ km}$.

Later, other authors reached for different conclusions after observing energy spectra in the low stratosphere, measured from experimental data recorded from commercial aircraft flights, Gage (1979), Lilly (1983), Nastrom and Gage (1985). Their picture suggested a 2D

turbulent inverse cascade, characterized by the $E(k) \sim k^{-5/3}$ spectrum, inside the interval of scales 100-1000 km.

More recently, Lindborg and Cho (2000, 2001a and 2001b) computed velocity spectra using data recorded during the MOZAIC program and also found a $k^{-5/3}$ spectrum. They suggested a dynamical mechanism different from 2D inverse cascade where energy is injected in the large scales by breaking Rossby-gravity waves and generates a chain process down to smaller scales. Their hypothesis is supported by the observation of a downscale energy flux, whereas 2D inverse cascade should exhibit upscale energy flux (Lindborg and Cho, 2000).

We wanted to reconsider this issue by performing a new analysis of the relative dispersion properties of the EOLE balloons within the framework of dynamical system theory. Relative dispersion properties are analyzed through the computation of the Finite-Scale Lyapunov Exponent, or shortly FSLE (Aurell et al. 1997, Artale et al. 1997, Boffetta et al. 2000a). The FSLE is based on the growth rate statistics of the distance between trajectories at fixed scale, and is a better tool at analyzing scale dependent properties than plain dispersion, as explained below. This new method has been already exploited for studies of relative dispersion in atmospheric and oceanic systems (Lacorata et al. 2001, Joseph and Legras 2002, Boffetta et al. 2001, LaCasce and Ohlmann 2003, Gioia et al. 2003) and also in laboratory convection experiments (Boffetta et al. 2000b).

This paper is organized as follows: in section II we describe the FSLE methodology; section III contains the results obtained from our analysis of the EOLE experimental data; in section IV we discuss the physical information that can be extracted from this paper and possible perspectives.

II. FINITE-SCALE RELATIVE DISPERSION

Generally speaking, most flows exhibit a range of scales over which fluid motion is expected to display different characteristics: a small-scale range where the velocity variations can be considered as a smooth function of space variables; a range of intermediate lengths corresponding to the coherent structures (and/or spatial fluctuations) present in the velocity field over which velocity variations are rough but highly correlated; a large-scale range over which spatial correlations have definitely decayed. In each of these ranges, relative dispersion between trajectories is governed by a different physical mechanism (chaos, turbu-

lence, diffusion) which can be, in principle, identified from the observations. In fully developed three-dimensional turbulence, motion is only smooth under the Kolmogorov dissipative scale. In the free stratified atmosphere (above the planetary boundary layer), turbulence is a relatively rare event: motion is most often smooth but for some localized convective or turbulent events, associated with mesoscale systems, that mix momentum and tracers. Hence one expects to find a smooth (chaotic) dispersion range ended at a scale characteristic of the spacing of mixing events, followed by a range covering the mesoscale to synoptic range, and finally standard diffusion at planetary scale. This view is supported by the ubiquitous observation of long-lived laminated structures in the free troposphere (Newell *et al.*, 1999).

In order to fix some terminology, we will use both symbols R and δ for indicating the distance between balloons: the former will be considered as a quantity function of time, the latter as an argument for scale-dependent functions.

A. *Diffusion and Chaos*

Diffusion is characterized in terms of diffusion coefficients, related to the elements of a diffusion tensor defined as

$$D_{ij} = \lim_{t \rightarrow \infty} \frac{1}{2t} \langle (x_i(t) - \langle x_i(0) \rangle)(x_j(t) - \langle x_j(0) \rangle) \rangle \quad (\text{II.1})$$

where $x_i(t)$ and $x_j(t)$ are the i -th and j -th coordinates at time t , with $i, j = 1, 2, 3$. The average operation $\langle \rangle$ is meant to be performed over a large number of particles. The diagonal elements are just the diffusion coefficients. When the D_{ii} 's are finite, then the diffusion is standard. This means that at long times, after the Lagrangian velocity correlations have decayed (Taylor, 1921), the variance of the particle displacement follows the law:

$$\langle ||\mathbf{x}(t) - \langle \mathbf{x}(0) \rangle||^2 \rangle \simeq 2Dt \quad (\text{II.2})$$

In presence of a velocity field characterized by coherent structures, it is more useful to observe the relative dispersion between the trajectories, rather than the absolute dispersion from the initial positions, given by (II.2), which is unavoidably dominated by the mean advection.

In the case of the EOLE experiment, where observing the expansion of balloon clusters with more than two elements is a rare event (ML) a measure of relative dispersion is given

by the mean square inter-particle distance:

$$\langle R^2(t) \rangle = \langle ||\mathbf{x}^{(m)}(t) - \mathbf{x}^{(n)}(t)||^2 \rangle \quad (\text{II.3})$$

averaged over all the pairs $(\mathbf{x}^{(m)}, \mathbf{x}^{(n)})$, where m and n label all the available N trajectories. Notice that the norm in (II.2) and (II.3) must be defined accordingly to the geometry of the fluid domain, i.e. in the atmosphere we use the arc distance on the great circle of the Earth connecting the two points. The quantity in (II.3) can be measured for both initially close pairs, balloons released from the same place at short time delay, and so-called *chance pairs*, balloons initially distant which come close to each other at a certain time and, later, spread away again (ML). Consistency of the average in eq. (II.3) requires all the trajectory pairs to have nearly the same initial distance, a condition which strongly limits the statistics. At long times, $\langle R(t)^2 \rangle$ defined in eq. (II.3) is expected to approach the function $4Dt$, where the 4 factor accounts for relative diffusion. When it happens that $\langle R(t)^2 \rangle \sim t^{2\nu}$ with $\nu > 1/2$, instead, the Lagrangian dispersion is considered as super-diffusion. A well-known example is the Richardson's law for the particle pair separation in 3D turbulence, for which $\nu = 3/2$ (Richardson 1926; Monin and Yanglom 1975).

On the other hand, in the limit of infinitesimal trajectory perturbations, much smaller than the characteristic lengths of the system, the evolution of the particle pair separation is characterized by the Lyapunov exponent (Lichtenberg and Lieberman, 1982), such that

$$\lambda = \lim_{t \rightarrow \infty} \lim_{R(0) \rightarrow 0} \frac{1}{t} \ln \frac{R(t)}{R(0)} \quad (\text{II.4})$$

If $\lambda > 0$ the growth is exponential and the motion is said chaotic. Chaos is a familiar manifestation of non linear dynamics, leading to strong stirring of trajectories (Ottino, 1989). The process, for example, of repeated filamentation around the polar vortex is basically due to Hamiltonian chaos (Legras and Dritschel, 1993). For finite perturbations within a smooth flow, the properties of exponential separation are observed for a finite time.

B. *Finite-Scale Lyapunov Exponent*

The idea of FSLE (Aurell et al. 1997; Artale et al. 1997), was formerly introduced in the framework of the dynamical systems theory, in order to characterize the growth of non-infinitesimal perturbations (i.e. the distance between trajectories). If δ is the scale of

the perturbation, and $\langle \tau(\delta) \rangle$ is the mean time that δ takes to grow a factor $r > 1$, then the FSLE is defined as

$$\lambda(\delta) = \frac{1}{\langle \tau(\delta) \rangle} \ln r \quad (\text{II.5})$$

The average operation is assumed to be performed over a large ensemble of realizations. For factors r not much larger than 1, $\lambda(\delta)$ does not depend sensitively on r . If $r = 2$ then $\langle \tau(\delta) \rangle$ is also called doubling time. Operatively, $N + 1$ scales are chosen to sample the spatial range of perturbation, $\delta_0 < \delta_1 < \dots < \delta_N$, and a growth factor r is defined such that $\delta_i = r \cdot \delta_{i-1}$ for $i = 1, N$. Let l_{min} and l_{max} be the smallest and the largest characteristic length of the system, respectively. If $\delta_0 \ll l_{min}$ then the FSLE characterizes the doubling time of infinitesimal perturbation. In the opposite side of the range, if $\delta_N \gg l_{max}$ then the FSLE follows the scaling law of diffusion $\lambda(\delta) \sim \delta^{-2}$ for $\delta \rightarrow \delta_N$, as can be deduced by noticing that the mean square particle distance must grow linearly in time, see (II.2). In general, if the mean square size of a tracer concentration follows the $\langle R^2 \rangle \sim t^{2\nu}$ law, the FSLE scales as $\lambda(\delta) \sim \delta^{-1/\nu}$. As we have seen before, for standard diffusion $\nu = 1/2$ while for Richardson's super-diffusion $\nu = 3/2$. The main interest of FSLE is to select processes occurring at a fixed scale. We stress that definition (II.5) differs substantially from

$$\lambda'(\delta) = \frac{1}{\langle R^2 \rangle} \frac{d\langle R^2 \rangle}{dt} \Big|_{\langle R^2 \rangle = \delta^2} \quad (\text{II.6})$$

defined in terms of the mean square relative displacement, because of the different averaging procedures in the two cases: $\langle R^2 \rangle$ is computed at fixed time while $\tau(\delta)$ is computed at fixed scale. As a result, a physical situation which is well characterized in terms of FSLE, either for scaling properties or the existence of transport barriers, may be less easily characterized by studying the time growth of trajectory separation (Boffetta et al., 2000b; Joseph and Legras, 2002). One reason is that $\langle R^2(t) \rangle$ depends on contribution from different regimes, as seen, for example in 3D turbulence where a dramatic dependence of $R^2(t)$ upon $R^2(0)$ is observed, even at very large Reynolds number (Fung *et al.*, 1992)

In cases where advection is strongly anisotropic, e.g. in presence of a structure like the stratospheric jet stream, it may be useful to define the FSLE in terms of meridional (cross-stream) displacement only:

$$\lambda_{mer}(\delta^{(mer)}) = \frac{1}{\langle \tau(\delta^{(mer)}) \rangle} \ln r \quad (\text{II.7})$$

where $\delta^{(mer)}$ is the latitude distance (or meridian arc) between two points.

Information about the relative dispersion properties are also extracted by another fixed-scale statistics, the Finite-Scale Relative Velocity (FSRV), named by analogy with FSLE, that is defined as

$$\nu_2(\delta) = \langle \delta \mathbf{v}(\delta)^2 \rangle \quad (\text{II.8})$$

where

$$\delta \mathbf{v}(\delta)^2 = (\dot{\mathbf{x}}^{(1)} - \dot{\mathbf{x}}^{(2)})^2 \quad (\text{II.9})$$

is the square Lagrangian velocity difference between two trajectories, $\mathbf{x}^{(1)}$ and $\mathbf{x}^{(2)}$, on scale δ , that is for $|\mathbf{x}^{(1)} - \mathbf{x}^{(2)}| = \delta$. The FSRV can be regarded as the 2nd order structure function of the Lagrangian velocity difference and provides a complementary analysis to the FSLE diagnostics. In particular, in the regime of Richardson's super-diffusion, the expected behavior for the FSRV is $\nu_2(\delta) \sim \delta^{2/3}$.

We report in the next section the results of our analysis.

III. ANALYSIS OF THE EOLE LAGRANGIAN DATA

After a preliminary data check, the number of balloons selected for the analysis has been reduced to 382. This has been obtained by discarding ambiguous ident numbers (some ident numbers have been used twice during the campaign), discarding trajectories that cross the equator and short tracks of less than 10 points.

Successive points along a balloon trajectory were mostly recorded at a time interval of 10^{-1} day (2.4 hours), but the overall distribution of the raw data does not cover uniformly the time axis. Hence, each of the coordinates (longitude and latitude) of every balloon trajectory has been interpolated in time by a cubic spline scheme, with a sampling rate of 25 points per day. Because of possible data impurities, each Lagrangian velocity value is monitored at every time step (0.04 day) and data segment with abnormally fast motions are discarded.

As pointed out by ML, a way to measure the dispersion between balloons is waiting for one of them to get close to another one, at a distance less than a threshold δ_0 , and then observing the evolution of their relative distance in time. This procedure is repeated for each balloon trajectory until the whole set of pairs is analyzed. The dataset includes original pairs of balloons that were launched within a short time interval and chance pairs of balloons meeting suddenly after a number of days. For the largest values of the threshold

used in this study, the number of chance pairs largely exceeds the number of original pairs. In this way, global properties of the Lagrangian transport are extracted from the contributions of balloon pairs randomly distributed all over the domain. The number of balloon pairs and its evolution as the separation crosses the N scales defined above is described by Table 1.

In Figure 1 four global relative dispersion curves are plotted, referring to four different initial thresholds $\delta_0 = 25$ km, 50 km, 100 km and 200 km. The statistical samples vary roughly in proportional way with δ_0 . Relative dispersion depends sensitively, as expected, on the initial conditions; the four curves meet together for separation larger than about 2500 km and saturation begins for separation larger than 4500 km, leaving room only for a short standard diffusive regime between these two separations and over a time duration of less than 10 days. The eddy diffusion coefficient, D_E , estimated by fitting the linear law $4D_E t$, results in $D_E \simeq 2.9 \cdot 10^6 \text{ m}^2\text{s}^{-1}$, a value compatible with what was found by ML. The pre-diffusive regime is not very clear, we can say that the behavior of the balloon separation looks like a power law with exponent (changing in time) between 3 and 1.

We report in Figure 2 the mean logarithmic growth of the balloon relative separation over all pairs selected by the threshold 25 km. At very short times (< 1 day) the slope corresponds to an exponential growth rate with e -folding time $\simeq 0.4$ day that we consider as a rough estimate of the LLE. At later times, the slope gradually decreases as the separation growth tends to a power law regime. In the same figure we also show the mean logarithmic growth of the inter-balloon distance computed for two 4-element clusters (that we label as 'A' and 'B'), launched with a time interval of 3 days between them. A linear behavior (exponential growth) for both clusters is observed for short intervals; we observe as the exponential regime lasts longer for the 'A' cluster ($\simeq 3$ days) than for the 'B' cluster ($\simeq 1$ days). This illustrates the fact that the duration of a dispersion regime, here the chaotic one, may exhibit large fluctuations generally due to different meteorological conditions. As a result, average time-dependent quantities, like $\langle R^2(t) \rangle$, sample different regimes at once and are poor diagnostics of dispersion properties. Incidentally, in ML the behavior of the relative dispersion between 100 and 1000 km is fitted by means of an exponential with characteristic e -folding time $\simeq 2.7$ days (see ML, figure 8), which is compatible with the growth rate of Figure 2 between the two horizontal lines marking the range 100-1000 km, if one wants to fit it with an exponential curve branch.

Figure 3 shows the global FSLE relatively to the same four initial thresholds used for the

relative dispersion and setting the amplification ratio r to $\sqrt{2}$. The main result of this study is that up to about 1000 km there is evidence of Richardson’s super-diffusion, compatible with a $k^{-5/3}$ spectrum, displayed by the behavior $\lambda(\delta) = \alpha\delta^{-2/3}$. The best fit is obtained for the initial thresholds 100 and 200 km which encompass a much larger number of pairs than smaller thresholds (see Table 1). The quantity α^3 is physically related to the mean relative kinetic energy growth rate (for unit mass) between balloons moving apart. Standard diffusion is approached at scales larger than 2000 km. The value of the eddy diffusion coefficient is estimated by fitting the FSLE in the diffusive range with $(4 \ln r)D_E\delta^{-2}$, as shown in Boffetta *et al.* (2000a) by means of a dimensional argument. We find that this value is $D_E \simeq 10^7 \text{ m}^2\text{s}^{-1}$. Notice that the initial threshold does not affect very much the general behavior, except for obvious changes in the statistical samples.

Figure 4 shows global (mainly zonal) and meridional (λ_{mer} , see (II.7)) FSLE of the balloon pairs with initial threshold 100 km. We find that the dispersion is basically isotropic up to scales of about 500 km, which is in rough agreement with the results of Morel and Larchevêque (they give a value three times larger but their analysis, see their Fig. 7, does not display a well-defined cut-off). At scales larger than 500 km, the two components of the FSLE decouple and the meridional dispersion rate follows the standard diffusion law $\sim \delta^{-2}$ with a meridional eddy diffusion coefficient $D_E \sim 10^6 \text{ m}^2\text{s}^{-1}$.

In order to compute the FSRV, the relative velocity between balloons is approximated by the finite difference formula $(|R(t + \Delta t)| - |R(t)|)/\Delta t$, where $|R(t)|$ is the absolute value of the great circle arc between two balloons at time t and $\Delta t = 0.04$ day is the time interval between two successive points along a trajectory. The properties of the Lagrangian relative velocity are shown in Figure 5. The FSRV confirms the results obtained with the FSLE: between 100 and 1000 km the behavior is $\sim \delta^{2/3}$, corresponding to the Richardson’s law; asymptotic saturation sets in beyond this range (fully uncorrelated velocities).

IV. DISCUSSION AND CONCLUSIONS

We have revisited the dispersion properties of the EOLE Lagrangian dataset using a new approach, using Finite-Scale Lyapunov Exponent, that is better suited to analyze scale dependent properties than standard tools that were used, e.g., by ML in a previous study of the same dataset. We were motivated by the fact that ML found results supporting a k^{-3}

inertial range between 100 and 1000 km, whereas more recent studies based on aircraft data found a $k^{-5/3}$ behavior in the same range of scales.

Our main result of our improved analysis is that the EOLE dataset supports a $k^{-5/3}$ behavior in the range 100-1000 km as shown by the scaling properties of FSLE in this range indicating Richardson's superdiffusion. At distances smaller than 100 km, our results suggest an exponential separation with an e-folding time of about one day, in rough agreement with ML. At scales larger 1000 km, the dispersion tends to a standard diffusion before saturating at the planetary scale. Since the large-scale flow is dominated by the meandering zonal circulation, estimated diffusion coefficient is 10 times larger for total dispersion ($10^7 \text{ m}^2\text{s}^{-1}$) than for meridional dispersion ($10^6 \text{ m}^2\text{s}^{-1}$).

Our result is compatible with an inverse 2D energy cascade in the range 100-1000 km or with the recently proposed alternative of a direct energy cascade (Lindborg and Cho, 2000). Our study of the EOLE experiment has shown that this still unparalleled dataset of Lagrangian trajectories in the atmosphere is in agreement with results obtained from aircraft data. The challenge is now to compare these trajectories with the global wind fields produced by the recent reanalysis by operational weather centers.

Acknowledgments

We warmly thank G. Boffetta, F. D'Andrea, V. Daniel, B. Joseph, A. Mazzino, F. Vial for interesting discussions and suggestions. G.L. thanks the European Science Foundation for financial support through a TAO Exchange Grant 1999, and the LMD-ENS (Paris) for hosting him.

-
- [] Aurell, E., G. Boffetta, A. Crisanti, G. Paladin, and A. Vulpiani, 1997: Predictability in the large: an extension of the concept of Lyapunov exponent. *J. Phys. A: Math. Gen.*, **30**, 1-26.
 - [] Artale, V., G. Boffetta, A. Celani, M. Cencini, and A. Vulpiani, 1997: Dispersion of passive tracers in closed basins: beyond the diffusion coefficient, *Phys. of Fluids*, **9**, 3162-3171.
 - [] Boffetta, G., A. Celani, M. Cencini, G. Lacorata, and A. Vulpiani, 2000a: Non-asymptotic properties of transport and mixing, *Chaos*, **10**, 1, 1-9.

- [] Boffetta, G., M. Cencini, S. Espa, and G. Querzoli, 2000b: Chaotic advection and relative dispersion in a convective flow, *Phys. Fluids*, **12**, 3160-3167.
- [] Boffetta, G., G. Lacorata, G. Redaelli, and A. Vulpiani, 2001: Barriers to transport: a review of different techniques, *Physica D*, **159**, 58-70.
- [] Fung, J.C.H., J.C.R. Hunt, N.A. Malik, and R.J. Perkins, 1992: Kinematic simulation of homogeneous turbulence by unsteady random fourier modes, *J. Fluid Mech.*, **236**, 281-318.
- [] Gage, K.S., 1979: Evidence for a $k^{-5/3}$ law inertial range in mesoscale two-dimensional turbulence, *J. of Atmos. Sci.*, **36**, 1950-1954.
- [] Gioia, G., G. Lacorata, E.P. Marques Filho, A. Mazzino, and U. Rizza, 2003: The Richardson's Law in Large-Eddy Simulations of Boundary Layer flows. Submitted to *Boundary Layer Meteor.*, <http://it.arxiv.org/find/nlin/1/Gioia/0/1/0/all/3/0>
- [] Joseph, B., and B. Legras, 2002: Relation between kinematic boundaries, stirring and barriers for the antarctic polar vortex, *J. of Atmos. Sci.*, **59**, 1198-1212.
- [] LaCasce, J.H., and C. Ohlmann, 2003: Relative dispersion at the surface of the Gulf of Mexico, *J. Mar. Res.*, **61**, 285-312.
- [] Lacorata, G., E. Aurell, and A. Vulpiani, 2001: Drifter dispersion in the Adriatic Sea: Lagrangian data and chaotic model, *Ann. Geophys.*, **19**, 121-129.
- [] Lichtenberg, A. J., and M. A. Lieberman, 1982: *Regular and stochastic motion* , Springer-Verlag, 655 pp.
- [] Lilly, D.K., 1983: Stratified turbulence and the mesoscale variability of the atmosphere, *J. Atmos. Sci.*, **40**, 749-761.
- [] Lindborg, E., and J.Y.N. Cho, 2000: Determining the cascade of passive scalars variance in the lower stratosphere, *Phys. Rev. Lett.*, **85**, 5663-5666.
- [] Lindborg E. and J.Y.N. Cho, 2001: Horizontal velocity structure functions in the upper troposphere and lower stratosphere 1. Observations, *J. Geophys. Res.*, **106**, 10223-10232.
- [] Lindborg, E., and J.Y.N. Cho, 2001: Horizontal velocity structure functions in the upper troposphere and lower stratosphere 2. Theoretical considerations, *J. Geophys. Res.*, **106**, 10233-10241.
- [] Monin, A.S., and A.M. Yaglom, 1975: Statistical Fluid Mechanics: Mechanics of Turbulence. Cambridge, MA/London, UK: MIT.
- [] Morel, P., and M. Desbois, 1974: Mean 200 mb circulation in the Southern Hemisphere deduced

- from EOLE balloon flights. *J. Atmos. Sci.*,**31**, 394-407.
- Morel, P., and M. Larchevêque, 1974: Relative dispersion of constant-level balloons in the 200 mb general circulation, *J. Atmos. Sci.*,**31**, 2189-2196.
 - Nastrom, G.D., 1985: A climatology of atmospheric wavenumber spectra of wind and temperature observed by commercial aircraft, *J. Atmos. Sci.*,**42**, 950-960.
 - Newell, R.E., V. Thouret, J. Y.N. Cho, P. Stoller, A. Marengo, and H.G. Smit, 1999: Ubiquity of quasi-horizontal layers in the troposphere, *Nature*,**398**, 316-319.
 - Ottino, J. M., 1989: The kinematics of mixing: stretching, chaos and transport, *Cambridge University Press* , 378 pp.
 - Richardson, L.F., 1926: Atmospheric diffusion shown on a distance-neighbor graph. *Proc. R. Soc. London Ser. A*,**110**, 709-737.
 - Taylor, G., 1921: Diffusion by continuous movement, *Proc. London Math. Soc.*,**20**, 196-212.

FIGURE CAPTIONS

Figure 1. Mean square balloon separation. The four curves refers to 4 different initial thresholds: 25 km (a), 50 km (b), 100 km (c) and 200 km (d). All the curves but for 25 km have been shifted in time in order to collapse together for $\langle R^2 \rangle > 10^7 \text{ km}^2$. The eddy diffusion coefficient corresponding to the indicated slope is $D_E \simeq 2.9 \cdot 10^6 \text{ m}^2\text{s}^{-1}$. Units: time in days, R^2 in km^2 .

Figure 2. Mean logarithmic growth of the balloon separation (+). The initial separation is $\leq 25 \text{ km}$. The two clusters 'A' (*) and 'B' (\times) have 4 balloons each and were launched with a 3-day lag in November 1971. The e -folding time of the exponential growth is $\simeq 0.4$ day. The two horizontal lines mark the range 100-1000 km (natural logarithm units). The straight line ML is the result found by Morel and Larchvêque (1974) in their fig. 8. Units: time in days, R in km.

Figure 3. FSLE of the balloon pairs, four curves with the same four initial thresholds as in Figure 1. The eddy diffusion coefficient is $D_E \simeq 10^7 \text{ m}^2\text{s}^{-1}$. The quantity α^3 gives the order of magnitude of the relative kinetic energy growth rate (for unit mass) between balloons in the Richardson's regime $\sim \delta^{-2/3}$. Units: δ in km, λ in day^{-1} .

Figure 4. FSLE of the balloon pairs, describing total (—) and meridional (\times) dispersion, with initial threshold 100 km. The meridional FSLE is λ_{mer} defined in (II.7). The meridional eddy diffusion coefficient is $D_E \simeq 1.5 \cdot 10^6 \text{ m}^2\text{s}^{-1}$. Units: δ in km, λ in day^{-1} .

Figure 5. FSRV of the balloon pairs for initial threshold 50 km. The reference velocity is $u_0 = 100 \text{ km/hour}$. The slope $2/3$ corresponds to the Richardson's law. Units: δ in km.

TABLE I: Number of balloon pairs analyzed for each scale during the computation of the FSLE. The first column is the order of the scale $\delta_n = r^n \delta_0$, with $r = \sqrt{2}$; the second, third, fourth and fifth column refer to the initial thresholds $\delta_0=25$ km, 50 km, 100 km and 200 km, respectively.

n	25 km	50 km	100 km	200 km
0	495	1037	2025	3979
1	344	782	1670	3649
2	391	867	1806	3699
3	414	895	1855	3764
4	440	951	1877	3722
5	442	955	1892	3687
6	456	950	1857	3563
7	442	944	1829	3471
8	448	928	1749	3327
9	440	906	1703	3131
10	428	865	1617	2648
11	418	845	1511	
12	397	794	1277	
13	389	756		
14	368	642		
15	346			
16	290			

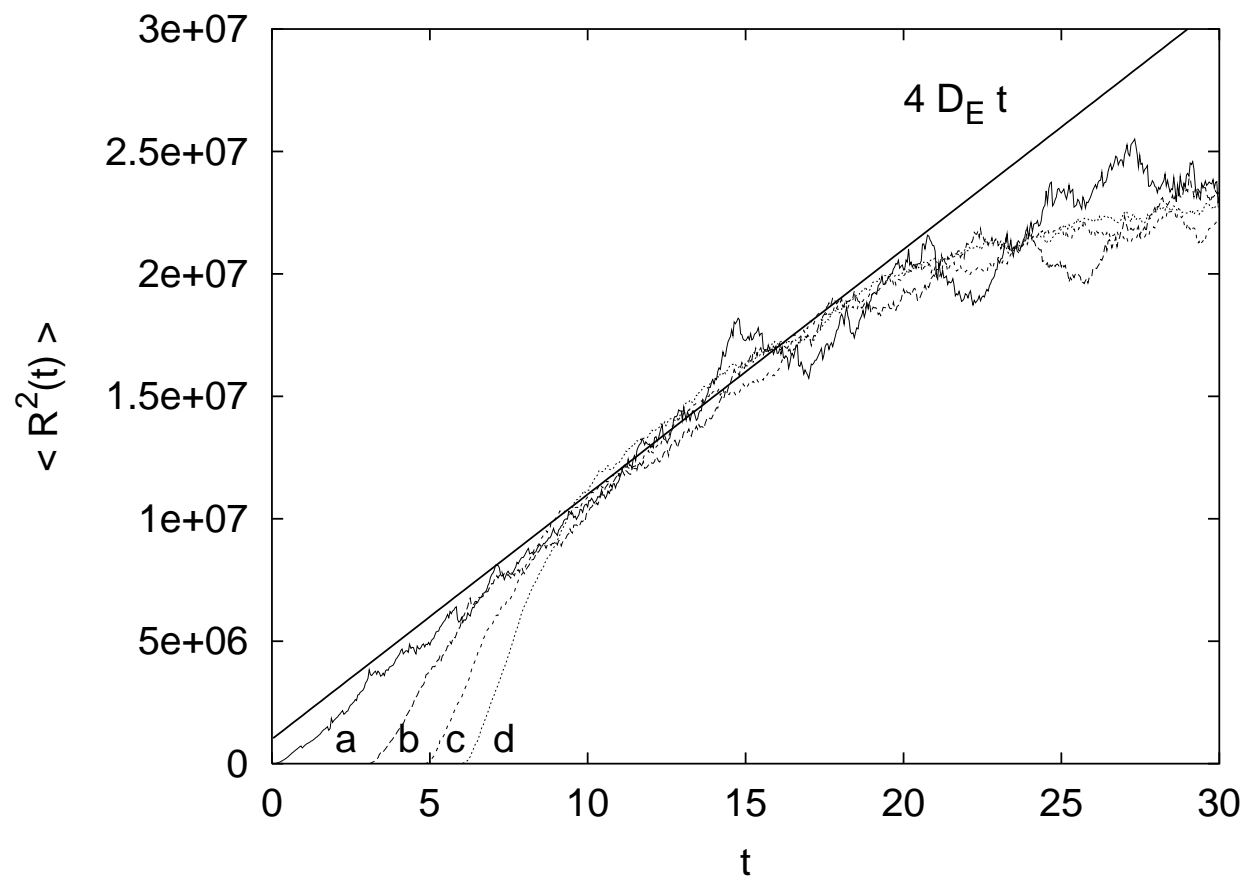


FIG. 1:

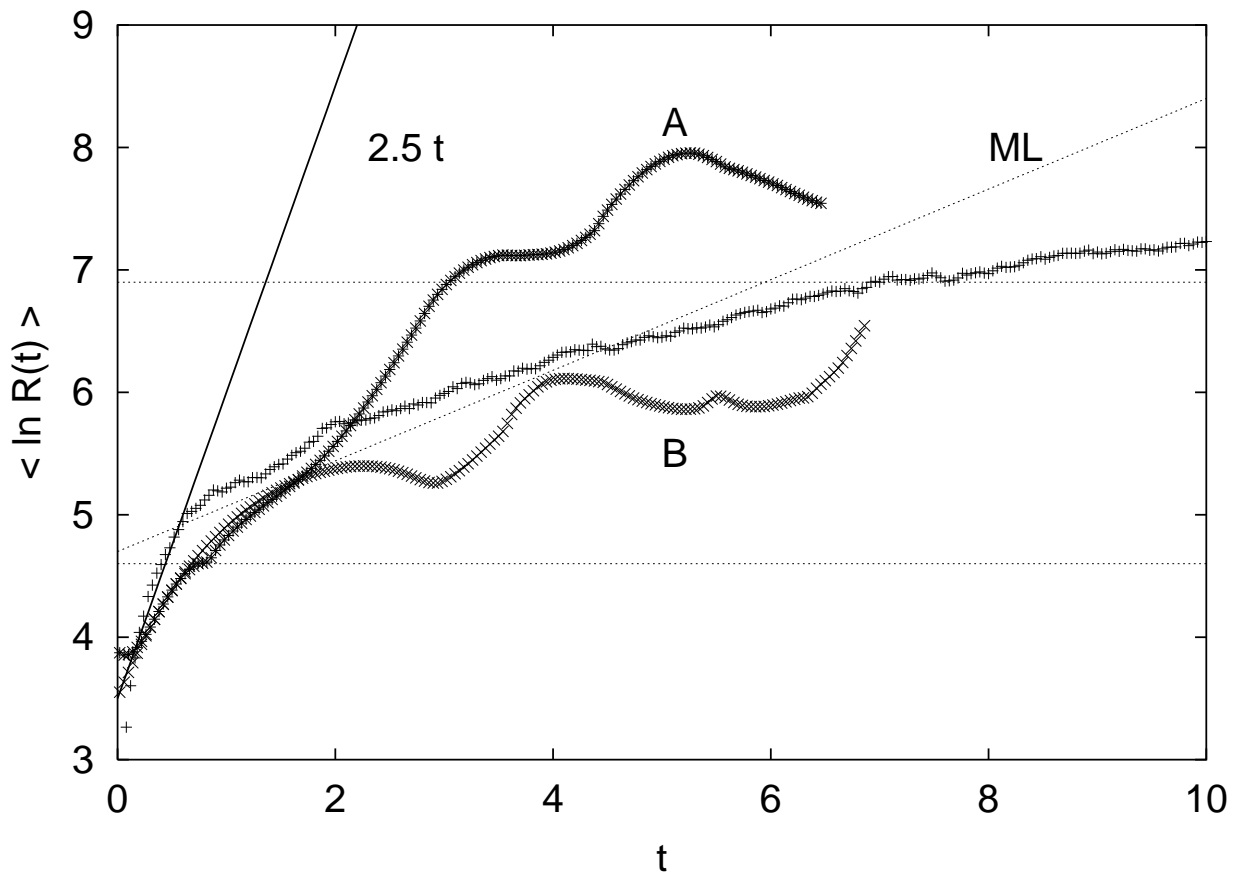


FIG. 2:

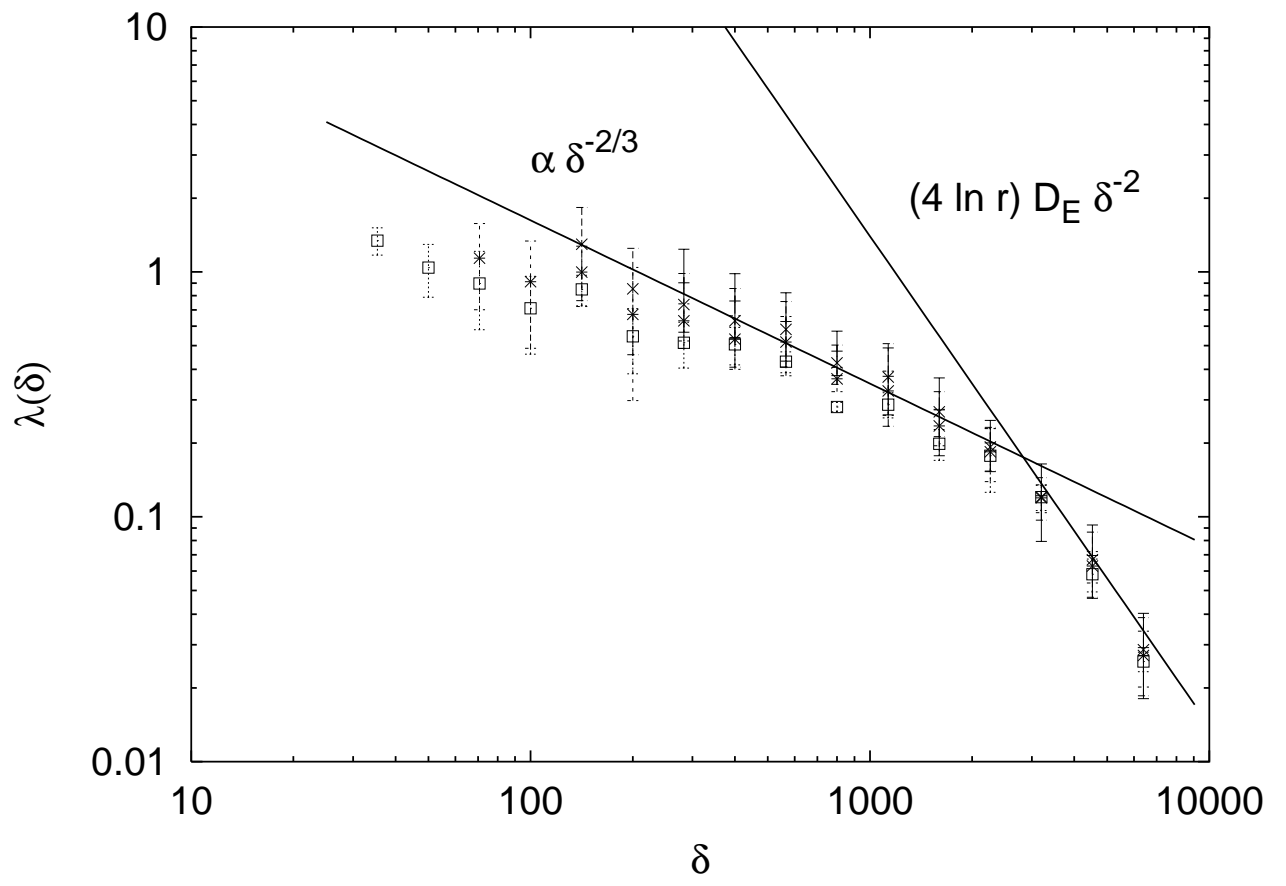


FIG. 3:

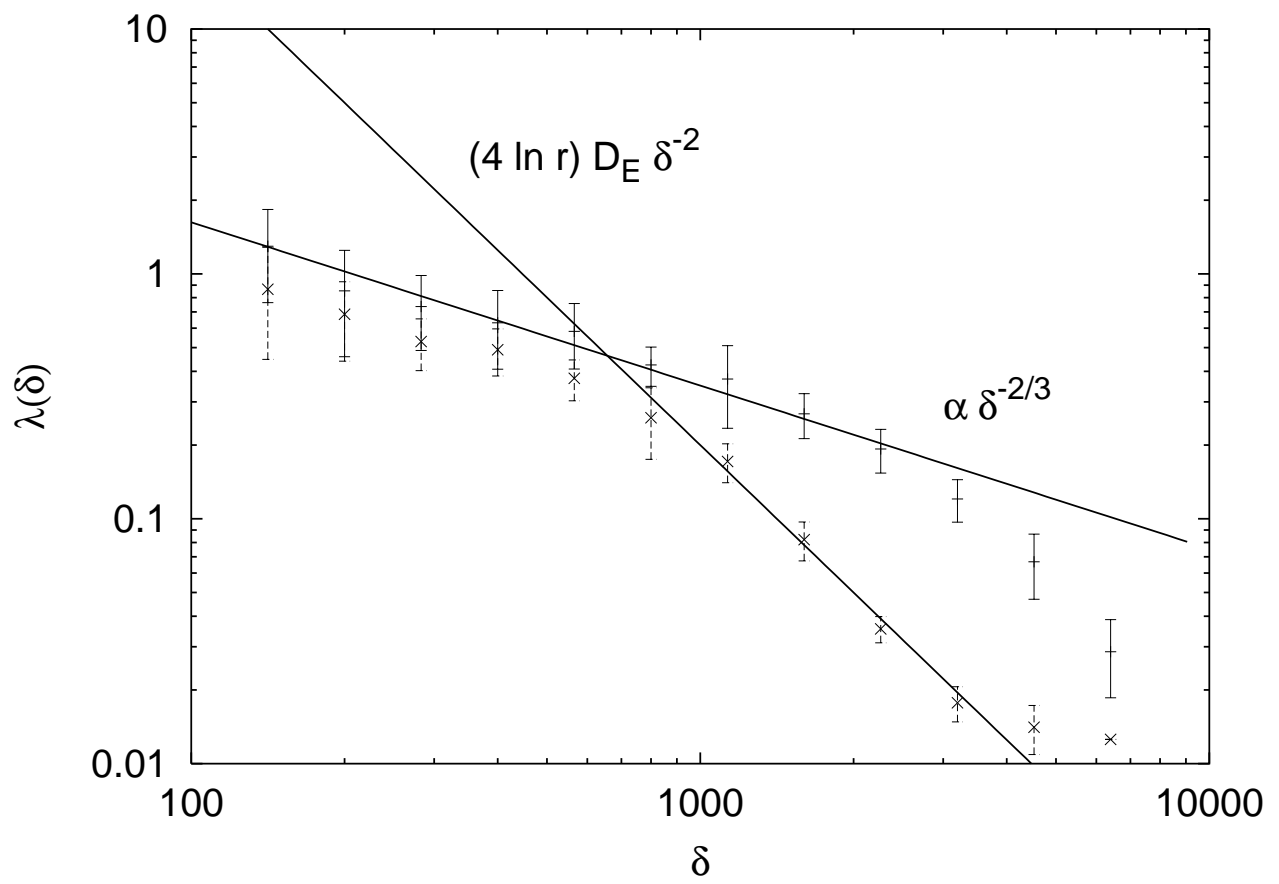


FIG. 4:

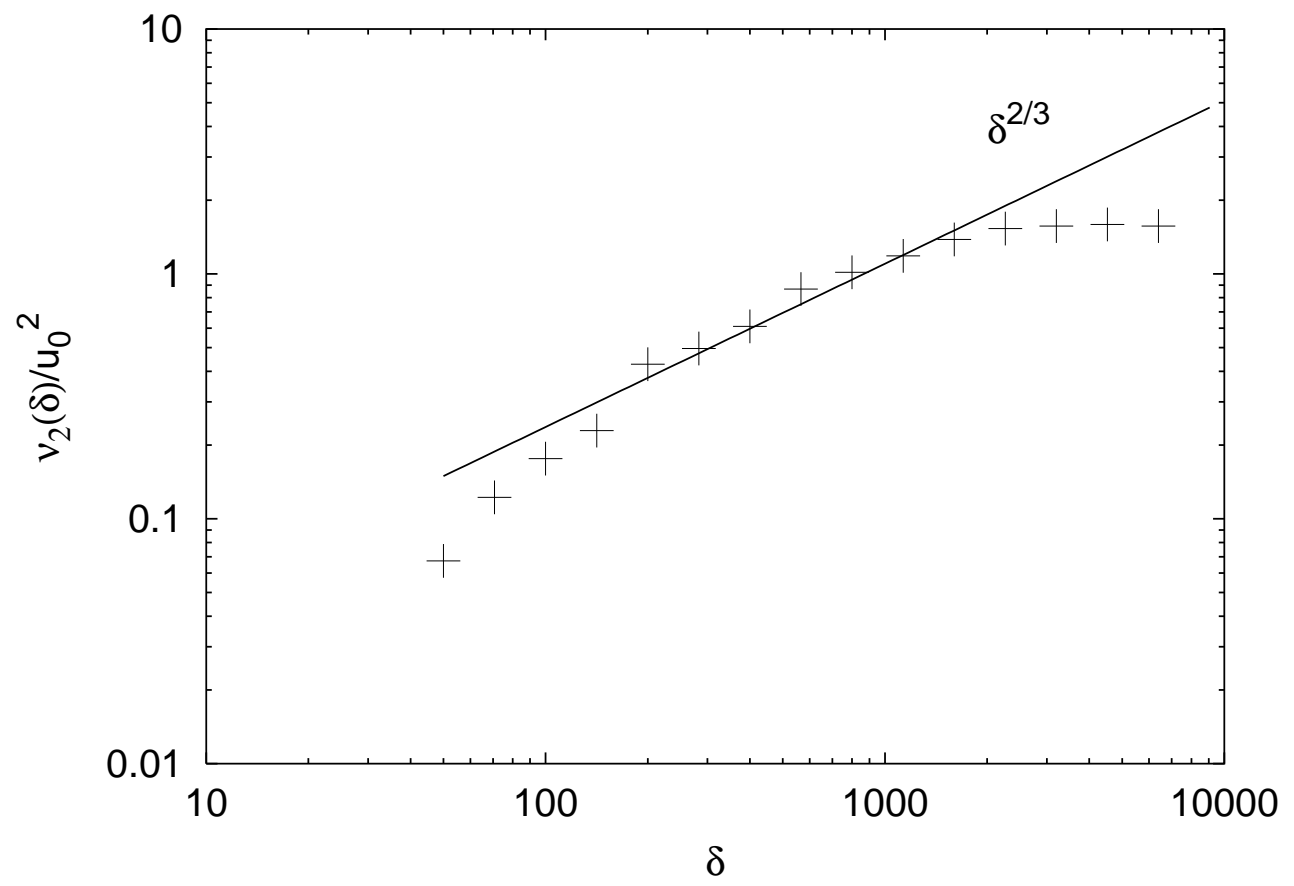


FIG. 5: